

# SCALING LAWS FOR THE MONTAGUE RESONANCE\*

I. Hofmann<sup>†</sup>, G. Franchetti, GSI, Darmstadt, Germany

## Abstract

We present scaling laws for the Montague-coupling resonance near  $2Q_x - 2Q_y = 0$  based on fully self-consistent particle-in-cell simulation (in the 2D coasting beam limit) and analytical theory. The scaling laws only contain the emittance ratio and the incoherent tune shift. For lattice design purpose they allow easy calculation of stop band widths, growth times and the effect for fast crossing of the stop-band. As an example, we apply the scaling laws to the tune diagram of the SIS100 synchrotron of the FAIR project, where avoidance of emittance exchange is crucial.

## INTRODUCTION

The space-charge-induced emittance coupling near the fourth order resonance condition  $2Q_x - 2Q_y = 0$ , the Montague resonance [1], is not only important for synchrotrons, but also for high-current linear accelerators as shown in Ref. [2]. There, the exchange can happen between the transverse and longitudinal degrees of freedom known as “equipartitioning”, but the 2D model exchange is still a good approximation [3].

For illustration we present an example for a specific set of parameters borrowed from measurements at the CERN Proton Synchrotron in the years 2002 and 2003 [4, 5]. We use a fixed vertical working point  $Q_{0,y} = 6.21$  and an emittance ratio of  $\epsilon_x/\epsilon_y = 3$ , while the absolute values of initial normalized rms emittances are chosen as  $\epsilon_x = 2.5\pi$  mm-mrad and  $\epsilon_y = 7.5\pi$  mm-mrad. The current is set to yield a maximum vertical tune shift of  $\Delta Q_y = -0.105$  in the center of a Gaussian distribution, which leads to a maximum horizontal tune shift of  $\Delta Q_x = -0.061$  for the given emittance ratio. Results are obtained with the MICROMAP-code [6] employing 50.000 particles and a 128x128 grid with conducting boundary conditions on a square box of width 6 times the horizontal rms size of the beam.

## SIMULATION EXAMPLES

The time behavior for two working points of the standard case under the assumption of a constant focusing and Gaussian input distribution is shown in Fig. 1. The rms emittance exchange (in units of  $\pi$  mm-mrad) increases, if  $Q_{0,x}$  is closer to  $Q_{0,y}$ . The rapid initial exchange is followed by emittance oscillations, which are slowly damped.

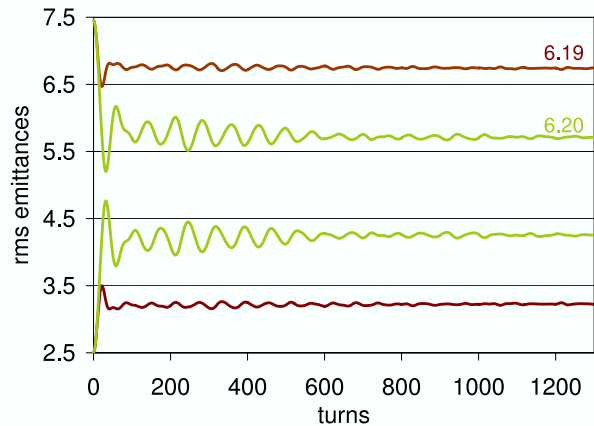


Figure 1: Time evolution of rms emittances for  $Q_{0,x} = 6.19, 6.20$  and  $Q_{0,y} = 6.21$ .

In Fig. 2 we show the final rms emittances by varying  $Q_{0,x}$  in small steps. The plotted values, where each marker is a simulation with different  $Q_{0,x}$ , are defined here and in all subsequent figures as averages of the rms emittance values between turn 1000 and 2000, which gives a good measure of the saturation stage. In order to justify the use

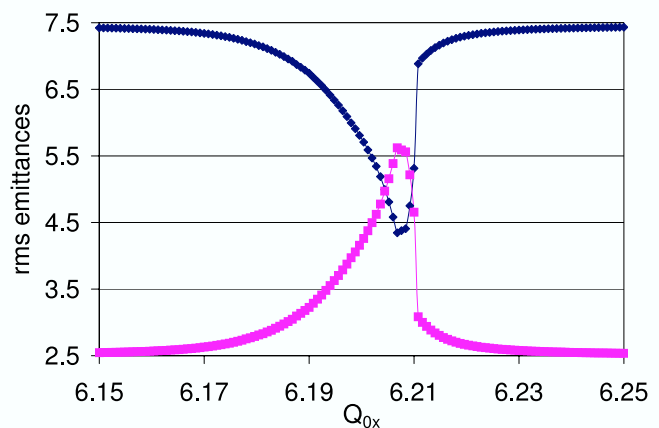


Figure 2: Final rms emittances for different values of  $Q_{0,x}$ .

\*Work supported by EU design study (contract 515873 - DIRACsecondary-Beams)

<sup>†</sup> i.hofmann@gsi.de

of constant focusing for the present study, we have compared it with (linear) periodic focusing and find that the difference is negligible.

## SCALING LAWS

The basis of the proposed scaling law for the stop-band width is a comparison of simulation results for different tune shifts and emittances with results from the dispersion relations derived from the analytical Vlasov theory for KV beams. Details of this comparison are presented in Ref. [5].

For relatively small tune shifts, as in circular machines, we characterize the effective stop band width by the width,  $\Theta$ , on the scale  $Q_{0,x}$  (for linacs with strong tune depression the expression is slightly modified [5]):

$$\Theta_{eff} = \frac{3}{2}(\sqrt{\epsilon_r} - 1)\Delta Q_x. \quad (1)$$

Note that  $\Delta Q_x$  is introduced here as space charge tune shift of an equivalent KV-beam, which is half the maximum tune shift of a Gaussian beam. Also,  $\epsilon_r > 1$  is understood here; if  $\epsilon_r < 1$ , Eq. 1 still holds if  $x$  is consistently replaced by  $y$ . “Effective” stop band width is understood here as extent of the region of “significant” exchange, where we disregard the points, where  $\leq 5\%$  of the maximum possible exchange occurs.

For practical applications the number of betatron periods,  $N_{ex}$ , after which the first exchange or crossover of emittances occurs, is of interest. By comparing simulations with different parameters, we have found that strictly  $N_{ex}^{-1} \propto \Delta Q_x / Q_{0,x}$  holds. Also,  $N_{ex}$  depends only on the emittance ratio,  $\epsilon_r$ , and not on the absolute value of emittances. The dependence on  $\epsilon_r$  in Gaussian beam simulations is relatively weak. In the range  $1.5 \leq \epsilon_r \leq 3$  a good fit to the simulation results is given by the simple expression, where  $\Delta Q_x$  is referring to the equivalent KV-beam tune depression:

$$N_{ex}^{-1} \approx \frac{\Delta Q_x}{Q_{0,x}}. \quad (2)$$

In a high-current linac with 50% tune depression by space charge, for example, hence  $\Delta Q_x / Q_{0,x} = 0.5$ , this suggests that the fastest exchange requires two (undepressed) betatron periods only. In a ring, instead,  $N_{ex}$  is typically in the range 20 - 100.

## DYNAMICAL CROSSING OF RESONANCES

In the previous sections we have discussed emittance coupling for fixed working points, which is the normal situation. This “static” case is substantially different from the case, where emittance exchange is achieved by slowly moving the tune across the resonance - the “dynamical” case.

The above  $N_{ex}$  also provides a guidance for what can be expected in case of a crossing of the stop band by a ramped tune. For slow crossing of the stop band, e.g.  $N \gg N_{ex}$ , the emittances are interchanged and the emittance ratio is basically inverted. For fast crossing the emittance exchange can be expected to be partial only, or negligible for very fast crossing with  $N \ll N_{ex}$ .

As an example for dynamical crossing we use the standard case of Fig. 2 and move the working point  $Q_{0,x}$  starting from the side of lower tunes over the range  $6.15 \leq$

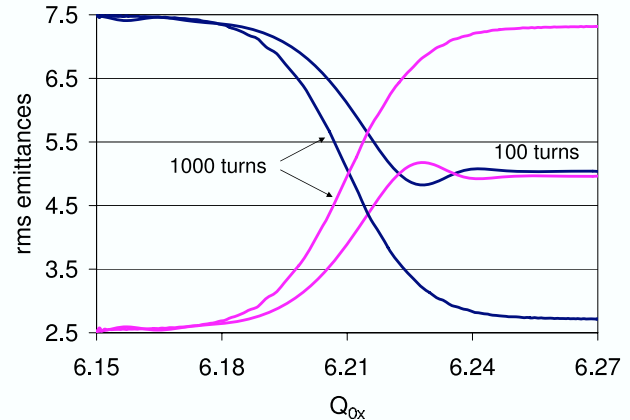


Figure 3: Evolution of emittances by crossing the stop-band dynamically from below over 100 and 1000 turns.

$Q_{0,x} \leq 6.27$  enclosing the stop-band. For this crossing “from below” we apply a linear tune ramp in time. In Fig. 3 we show the evolution of emittances as function of the instantaneous tune for two cases, where the crossing of the same tune range is performed in 100, respectively 1000 turns. It is noted that for the 100 turns case the final emittances are practically equal; for the 1000 turns case the final emittances are basically exchanged with the initial emittances.

The complete picture of the final emittances after crossing the band at variable number of turns is shown in Fig. 4. In the 100 turns case the essential part of the stop-band in

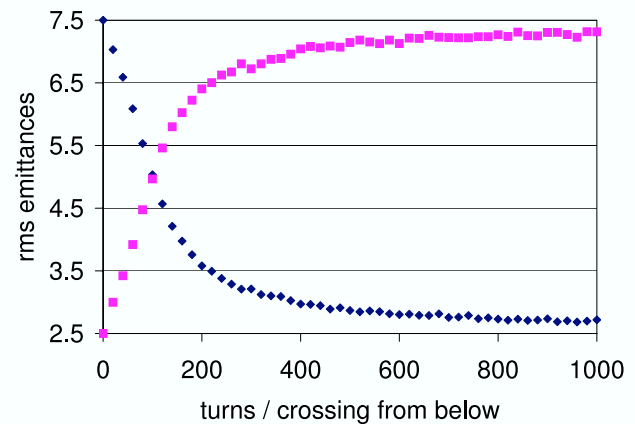


Figure 4: Final emittances after crossing  $Q_{0,x} = 6.15 \rightarrow 6.27$  at variable rates.

Fig. 2, which has a tune width of 0.04, is crossed in 33 turns or 205 betatron periods. This time agrees with the

fastest rise time of the static case, which therefore sets the time-scale needed for a crossing to just equalize final emittances. Note that for faster crossing the exchange is only partial, with a linear dependence on the number of turns. Hence we find that with  $N < N_{ex}$  the emittance exchange is proportional to the inverse tune changing rate. For fixed tune changing rate the emittance change depends quadratically on the tune shift due to the fact that both, the stop band width and the growth rate (in the center of the stop band) increase linearly with  $\Delta Q_x$ . Defining  $\dot{Q}$  as tune change per turn, we thus find that the emittance change follows

$$\Delta\epsilon \propto \frac{(\Delta Q_x)^2}{\dot{Q}}, \quad (3)$$

assuming that the full stop-band is crossed at constant rate.

Crossing in the opposite direction leads to a significantly suppressed emittance coupling due to the fact that the space charge de-tuning points downwards in the tune diagram (details see Ref. [5]).

## APPLICATION TO THE SIS100

The high-current working point of the SIS100 (WP1) is not split by an integer [7]. Therefore, it has to be chosen at a safe distance from the diagonal to avoid emittance exchange due to the Montague resonance. With the nominal emittance ratio  $\epsilon_r = 2.5$  and an upper limit for the full tune spread of  $\Delta Q_y = -0.3$  for a Gaussian beam, we obtain from Eq. 1 a stop band width (in the direction of  $Q_{0,x}$ ) of 0.13 to the left of the diagonal. This one-sided location of the stop band is due to  $\epsilon_x > \epsilon_y$  - a reversal would make the stop band flip around the axis.

Here it is appropriate to introduce a safety margin to take into account that the above idealized theoretical results have been obtained under idealized conditions ignoring synchrotron motion, dispersion and possibly other effects (like residual linear coupling). A comparison of Eq. 1 with measurements taken at the CERN Proton Synchrotron in 2003 [4] for a similar emittance ratio suggests that the edges of the measured stop bands are softer and extend to about  $\pm 50\%$  of the idealized stop band on each side. We therefore adopt a doubling of the stop band of Eq. 1 as safety margin, with the understanding that it is expanded on each side by 50%. The resulting stop band of width 0.26 is shown in Fig. 5. Note that without the safety margin the stop band would entirely be above the diagonal.

Closer to the integers we expect troubles with resistive wall instabilities, hence the Montague stop band together with the resistive wall limitation limits the working point flexibility. An acceptable compromise for the SIS100 is given by  $Q_{0,x} = 18.84$  and  $Q_{0,y} = 18.73$ , but this requires compensation of the half-integer resonance; for smaller tune spread, e.g.  $\Delta Q_y = -0.2$ , such a compensation is avoidable.

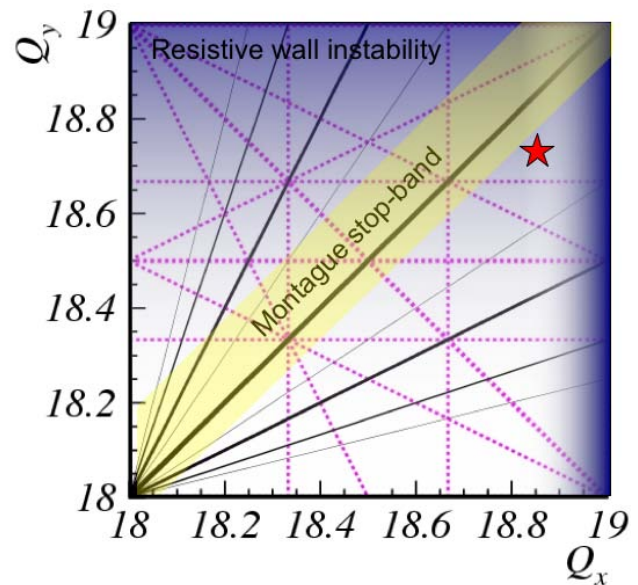


Figure 5: Montague resonance stop band for SIS100 including  $\pm 50\%$  safety margin and proposed working point WP1.

## OUTLOOK

The space charge driven “Montague” coupling resonance is an example of a purely space charge driven resonance, which can be described by relatively simple scaling laws for practical applications. Due to its significant strength the Montague resonance cannot be compensated. For future work more experimental data and simulations under realistic conditions would be desirable to obtain a broader basis for the safety margin, which was introduced here as  $\pm 50\%$ .

## REFERENCES

- [1] B.W. Montague, CERN-Report No. 68-38, CERN, 1968.
- [2] I. Hofmann, G. Franchetti, J. Qiang, R. Ryne, F. Gerigk, D. Jeon and N. Pichoff, *Proceedings of the European Accelerator Conference*, Paris, 2002, ed. J.L. Laclare, p. 74 (2002).
- [3] I. Hofmann, G. Franchetti, O. Boine-Frankenheim, J. Qiang and R. D. Ryne, *Phys. Rev. ST Accel. Beams* **6**, 024202 (2003).
- [4] E. Metral et. al., *AIP Conf. Proc.* **773**, New York (ed. I. Hofmann et al.), 2004, p. 122
- [5] I. Hofmann and G. Franchetti, *Phys. Rev. ST Accel. Beams* **69**, 054202 (2006).
- [6] G. Franchetti, I. Hofmann, and G. Turchetti *AIP Conf. Proc.* **448**, 233 (1998); ed. A.U. Luccio and W.T. Weng.
- [7] G. Franchetti et al., paper THPCH005, these Proceedings